Beyond Lambertian light trapping for large-area silicon solar cells: fabrication methods

Jovan Maksimovic[1†], Jingwen Hu[1†], Soon Hock Ng[1], Tomas Katkus[1], Gediminas Seniutinas[1], Tatiana Pinedo Rivera[2], Michael Stuiber[2], Yoshiaki Nishijima[3,4], Sajeev John[5]* and Saulius Juodkazis ⓘ[1,6]*

[1]Optical Sciences Centre and ARC Training Centre in Surface Engineering for Advanced Materials (SEAM), School of Science, Swinburne University of Technology, Hawthorn Vic 3122, Australia; [2]Melbourne Centre for Nanofabrication, ANFF Victoria, 151 Wellington Rd., Clayton Vic 3168 Australia; [3]Department of Electrical and Computer Engineering, Graduate School of Engineering, Yokohama National University, 79-5 Tokiwadai, Hodogaya-ku, Yokohama 240-8501, Japan; [4]Institute of Advanced Sciences, Yokohama National University, 79-5 Tokiwadai, Hodogaya-ku, Yokohama 240-8501, Japan; [5]Department of Physics, University of Toronto, 60 St. George Street, Toronto, ON, M5S 1A7, Canada; [6]World Research Hub Initiative (WRHI), School of Materials and Chemical Technology, Tokyo Institute of Technology, 2-12-1, Ookayama, Meguro-ku, Tokyo 152-8550, Japan.

†These authors contributed equally to this work.

*Correspondence: S John, E-mail: John@physics.utoronto.ca; S Juodkazis, E-mail: SJuodkazis@swin.edu.au

Supplementary information for this paper is available at https://doi.org/10.29026/oea.2022.210086
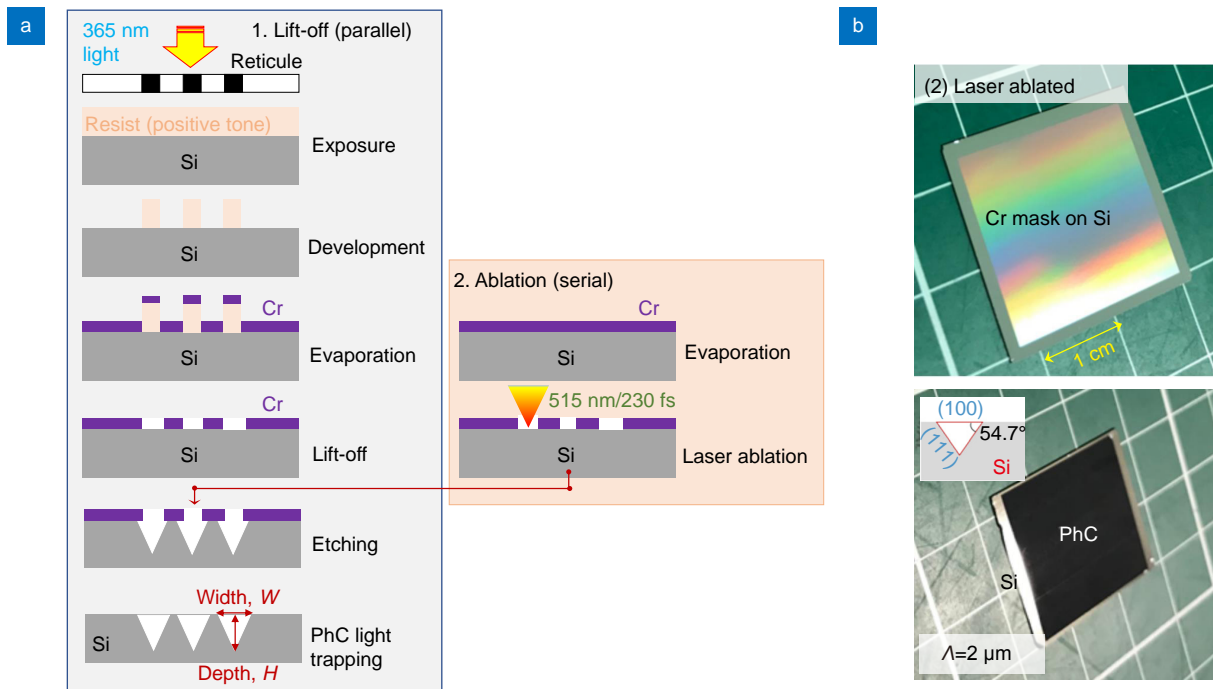
Fig. S1 | (**a**) A flow chart of processing steps required to fabricate light trapping PhC: 1) lift-off (parallel) and 2) ablation (serial) pathways. Projection stepper lithography (a-1) was used with 5× demagnification. (**b**) Images of laser ablated mask and the final plasma etched PhC pattern with Λ = 2 µm period.
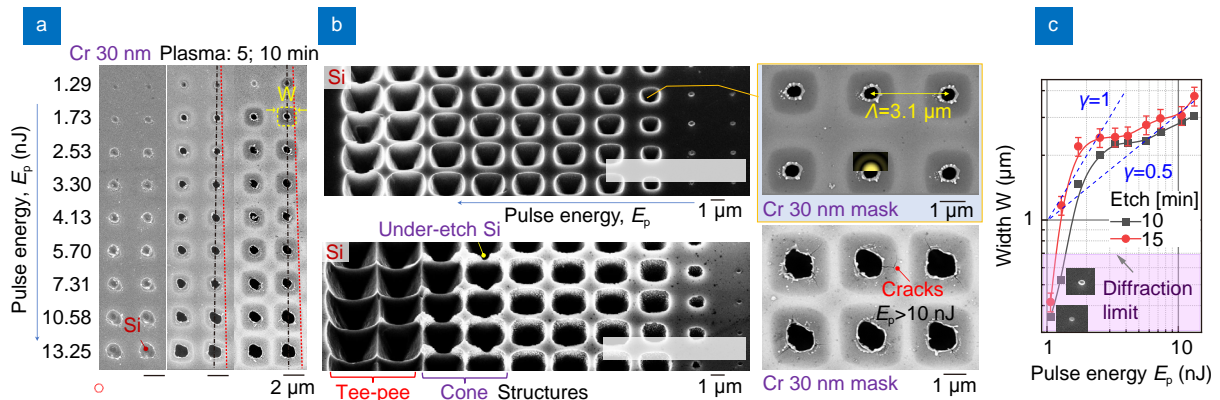
Fig. S2 | Etch through the Cr-mask defined by direct laser writing. (**a**) SEM images of laser ablated and plasma etched samples. (**b**) SEM image of Si after plasma etching for 10 and 15 min and Cr-mask removal; right-side: Cr-mask after plasma etch. (**c**) Width W evolution for different diameter D of the mask opening (E_p energy); data from (b) where the horizontal measure of the hole was used for the W. Plasma etch: SF_6:CHF_3:O_2 at 5:1:1 flow rate ratio. The SEM insets shows surface modification for small E_p where Si:Cr alloying occurred. Slope exponents γ = 1, 0.5 corresponds to the linear and diffusion $\propto \sqrt{D \times time}$ defined processes, where D [cm²/s] is diffusion coefficient, respectively.

A flow chart of PhC fabrication on Si surface is shown in Fig. S1(a) and the final result for fs-laser fabrication in (b). Figure S2 summarises structural changes during plasma etching through different diameter D holes which were laser ablated through Cr film. Different reactive ion etching (RIE) protocols were tested with a Cr mask with $\sim$ 200 nm holes obtained using a stepper lithography followed by lift-off (Fig. 5). An optimised RIE procedure to obtain etched pits with the aspect ratio close to one was carried out at flow rates of SF_6 50 sccm, CHF_3 10 sccm, O_2 10 sccm (at bias 5 W) for 7 min; the inductively coupled plasma (ICP) power was 180 W, pressure 5 Pa ($\sim$ 37.5 mTorr). It is noteworthy that the aspect ratio of KOH etch Si is 0.71 for the inverted pyramids on Si(100) surface. Figure S4 shows SEM images of etched patterns after removal of Cr mask. By defining the opening width of the etched Si pit, W, ratio to the period of the pattern, Λ, it is possible to establish the required etching protocol. Final PhC pattern should have minimum width of the ridges R between adjacent etched inverted pyramids, which corresponds to the condition $W/\Lambda = 1$ or $W + R' = \Lambda$.
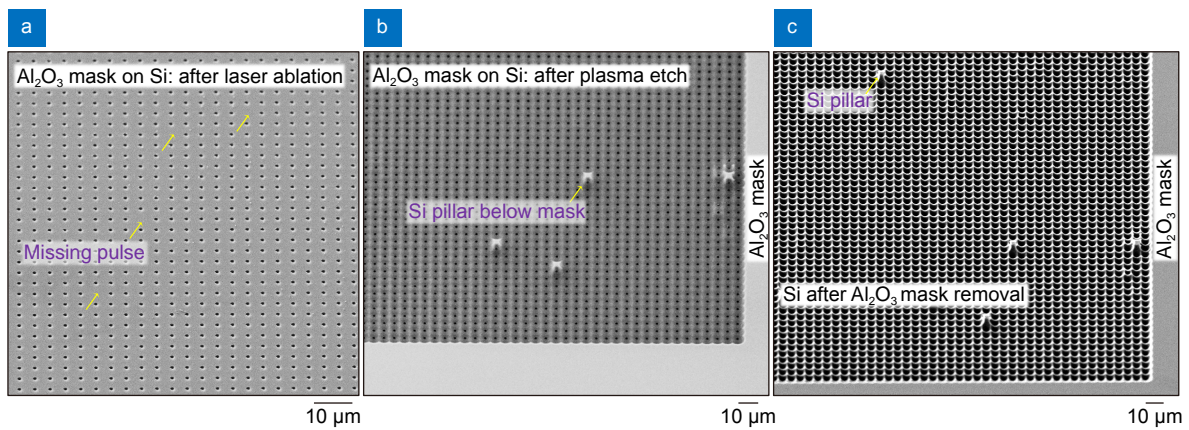
Fig. S3 | Alumina Al₂O₃ (20 nm thickness) on Si as a hard mask for plasma etching; Al₂O₃ deposition was made by e-beam evaporation.
(**a**) SEM images of laser ablated holes in Al₂O₃ by 515 nm/230 fs pusles of energy E_p = 12.5 nJ (at focus). (**b**) Plasma etched PhC texture at the under-etch conditions (etched protocol was same as for the Cr-mask; Fig. S2). (**c**) Surface of Si after Al₂O₃ mask is removed by ultrasonication in acetone. Upright pyramid is formed with under-etch conditions when an opening in the mask is missing (marked by arrows).
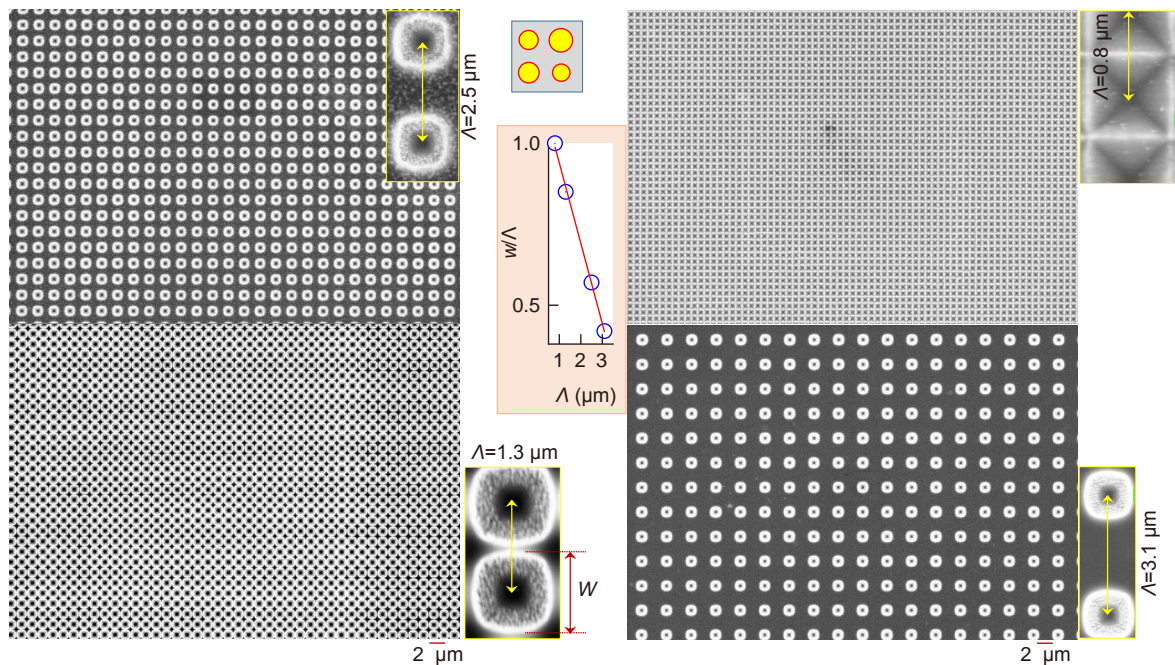
Fig. S4 | Reactive ion etching of PhC patterns on Si. SEM images of four-segments after etching and removal of Cr mask (see, Figure 5 for the geometry). Insets for each pattern shows a closeup view of one period of the PhC structure (magnifications of the insets differ). The center plot-inset shows linear scaling of the under-etch ratio W/Λ vs. period Λ. RIE conditions were: SF₆ 50 sccm, CHF₃ 10 sccm, O₂ 10 sccm (at bias 5 W) for 7 min.

Inset plot in Fig. S4 shows a linear dependence for the $W/\Lambda = f(\Lambda)$ for the patterns etched in the same run at the etch time of $t_{etch} = 7$ min. The shape of plasma etched inverted pyramids was apparently different (Fig. S4) resembling KOH-etched shape defined by the crystalline structure of Si for $\Lambda = 0.8$ μm while showing tee-pee structure for larger Λ.

Figure S5 shows results of Si initially etched by RIE then with different dry and wet etching treatments applied. It was observed that with the smallest pulse energy of $E_p \approx 1$ nJ, there were no ablation opening but a noticeable surface modification took place. Plasma etching, which produced a nanotextured black-Si surface was applied to reveal structural modifications on the Cr mask at the low energy laser pulses (see Fig. S5(b)). Those regions acted as a mask and prevented surface etching. The mask is expected to be Si:Cr nano-alloy which can have different compositions depending on the formation at the higher temperatures close to the Cr melting at 1860 °C or that of Si at 1414 °C[41]. As shown in Section *Results*, the largest part of laser pulse energy 91 % is deposited into Cr. Hence high temperature phases of Cr-rich

alloy are expected Cr_3Si, β-Cr_5Si_3 and α-Cr_5Si_3[41] since they are formed at higher temperatures. However, due to an ultra-fast thermal quenching of the alloy due to a very small volume, formation of non-equilibrium phases of the melt are possible, as was observed for bulk damage of materials with ultra-short laser pulses[42]. In such a case, Si-rich phases are also possible since they are formed at lower temperatures (closer to the Si-Cr interface): $CrSi$ and $CrSi_2$; interestingly, the latter is a thermoelectric material[41]. Phases such as amorphous-Al_2O_3, which are not existent at room conditions, can be formed under tightly focused fs-laser pulses[43], hence an amorphous Si:Cr nano-alloys can be expected. A separate study is planned to investigate nano-alloy formation at the conditions used.
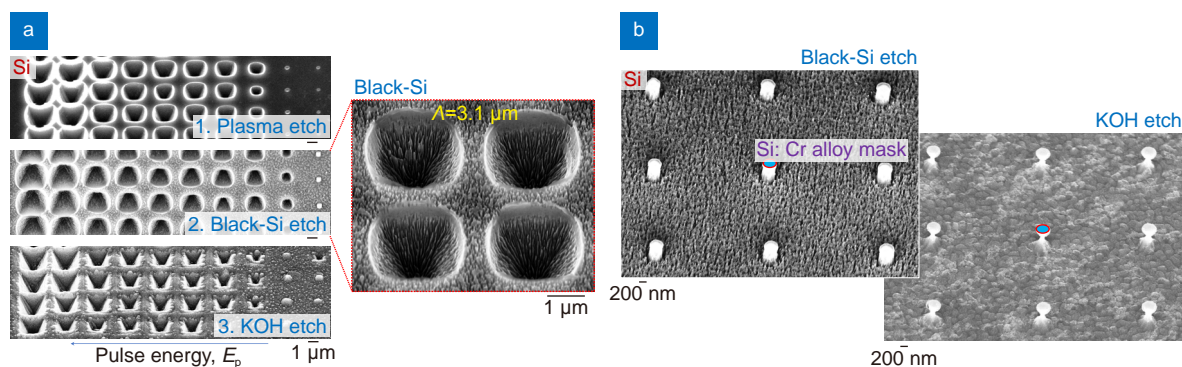
Fig. S5 | Si:Cr alloy formed at low pulse energies $E_p \approx 1$ nJ. (**a**) SEM images of Si after subsequent etching steps: 1) plasma (as in Fig. S2), 2) black Si etch (5 min), 3) KOH (5–10 min). (**b**) Formation of Si:Cr alloy at low laser pulse energy irradiation of Cr mask was best revealed by black-Si etch step and subsequent KOH etch.